

*International Journal Of*  
**Recent Scientific  
Research**

ISSN: 0976-3031  
Volume: 7(6) June -2016

CHEMICAL PREPARATION, THERMAL BEHAVIOR, KINETIC, IR STUDIES OF  $\text{CdK}_4(\text{P}_3\text{O}_9)_2 \cdot 2\text{H}_2\text{O}$ , CRYSTALLOGRAPHIC DATA OF A NEW CYCLOTRIPHOSPHATE  
 $\text{CdK}_4(\text{P}_3\text{O}_9)_2$  NEW FERTILIZER TYPE KP

El Kababi K., Atibi A., Belhabra M., Zerraf S., Fahim I.,  
Tridane M., Bassiri M and Belaaouad S



THE OFFICIAL PUBLICATION OF  
INTERNATIONAL JOURNAL OF RECENT SCIENTIFIC RESEARCH (IJRSR)  
<http://www.recentscientific.com/> [recentscientific@gmail.com](mailto:recentscientific@gmail.com)



ISSN: 0976-3031

Available Online at <http://www.recentscientific.com>

International Journal of Recent Scientific Research  
Vol. 7, Issue, 6, pp. 11793-11800, June, 2016

**International Journal of  
Recent Scientific  
Research**

## Research Article

### CHEMICAL PREPARATION, THERMAL BEHAVIOR, KINETIC, IR STUDIES OF $\text{CdK}_4(\text{P}_3\text{O}_9)_2 \cdot 2\text{H}_2\text{O}$ , CRYSTALLOGRAPHIC DATA OF A NEW CYCLOTRIPHOSPHATE $\text{CdK}_4(\text{P}_3\text{O}_9)_2$ NEW FERTILIZER TYPE KP

El Kababi K<sup>1,2</sup>, Atibi A<sup>1,2</sup>, Belhabra M<sup>1</sup>, Zerraf S<sup>1</sup>, Fahim I<sup>1</sup>,  
Tridane M<sup>1,2</sup>, Bassiri M<sup>1</sup> and Belaaouad S<sup>1</sup>

<sup>1</sup>Laboratoire de Chimie-Physique des Matériaux, Faculté des Sciences  
Ben M'sik, B. P. 7955. Casablanca. Maroc

<sup>2</sup>Centre Régional des métiers d'enseignement et de formation Casablanca  
Anfa Bd Bir Anzarane Casablanca. Maroc

#### ARTICLE INFO

##### Article History:

Received 05<sup>th</sup> March, 2016

Received in revised form 08<sup>th</sup> April, 2016

Accepted 10<sup>th</sup> May, 2016

Published online 28<sup>st</sup> June, 2016

##### Key Words:

Chemical preparation, thermal behavior, infrared spectrometry, thermal analyses (TGA-DTA), differential scanning calorimetry (DSC), X-ray diffraction.

#### ABSTRACT

Chemical preparation, thermal behavior and IR studies are given for the cyclotriphosphate  $\text{CdK}_4(\text{P}_3\text{O}_9)_2 \cdot 2\text{H}_2\text{O}$  and its anhydrous form  $\text{CdK}_4(\text{P}_3\text{O}_9)_2$ .  $\text{CdK}_4(\text{P}_3\text{O}_9)_2 \cdot 2\text{H}_2\text{O}$ , isotypic to  $\text{MnK}_4(\text{P}_3\text{O}_9)_2 \cdot 2\text{H}_2\text{O}$ , is triclinic P-1 with the following unit-cell dimensions:  $a = 9.235(4)\text{\AA}$ ,  $b = 7.599(3)\text{\AA}$ ,  $c = 7.148(1)\text{\AA}$ ,  $\alpha = 96.38(2)^\circ$ ,  $\beta = 103.90(5)^\circ$ ,  $\gamma = 102.06(3)^\circ$  and  $Z = 1$ . The total dehydration of  $\text{CdK}_4(\text{P}_3\text{O}_9)_2 \cdot 2\text{H}_2\text{O}$ , between  $350^\circ\text{C}$  and  $420^\circ\text{C}$ , leads to its anhydrous form  $\text{CdK}_4(\text{P}_3\text{O}_9)_2$ .  $\text{CdK}_4(\text{P}_3\text{O}_9)_2$  is a new cyclotriphosphate crystallizing in the rhombohedral system, space group  $\text{P}\bar{3}_1\text{c}$ ,  $Z = 2$  with the following unit-cell dimensions:  $a = b = 7.337(3)\text{\AA}$  and  $c = 19.920(1)\text{\AA}$ .  $\text{CdK}_4(\text{P}_3\text{O}_9)_2$  is stable until its melting point at  $431^\circ\text{C}$ . The thermal behavior of  $\text{CdK}_4(\text{P}_3\text{O}_9)_2 \cdot 2\text{H}_2\text{O}$  has been investigated and interpreted by comparison with IR absorption spectrometry and X-ray diffraction experiments. Two different methods Ozawa and KAS have been selected in studying the kinetics of thermal behavior of the title compound.

**Copyright © El Kababi K et al., 2016**, this is an open-access article distributed under the terms of the Creative Commons Attribution License, which permits unrestricted use, distribution and reproduction in any medium, provided the original work is properly cited.

## INTRODUCTION

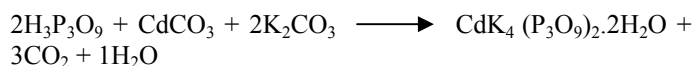
During a systematic investigation of cyclotriphosphates of monovalent cations  $\text{M}^I$  ( $\text{M}^I = \text{Na}^+$ ,  $\text{K}^+$ ,  $\text{Ag}^+$  and  $\text{NH}_4^+$ ), manganese and cadmium, a new form of the potassium and cadmium salt  $\text{CdK}_4(\text{P}_3\text{O}_9)_2$  has been obtained. Three cyclotriphosphates  $\text{MnNa}_4(\text{P}_3\text{O}_9)_2 \cdot 4\text{H}_2\text{O}$  [1,2,3],  $\text{Mn}(\text{NH}_4)_4(\text{P}_3\text{O}_9)_2 \cdot 6\text{H}_2\text{O}$  [3],  $\text{MnK}_4(\text{P}_3\text{O}_9)_2 \cdot 2\text{H}_2\text{O}$  and  $\text{MnAg}_4(\text{P}_3\text{O}_9)_2 \cdot 6\text{H}_2\text{O}$  [4, 5] have already been prepared and characterized. The present work reports the chemical preparation, thermal behavior, IR studies of  $\text{CdK}_4(\text{P}_3\text{O}_9)_2 \cdot 2\text{H}_2\text{O}$  and its anhydrous form  $\text{CdK}_4(\text{P}_3\text{O}_9)_2$  and crystallographic data of  $\text{CdK}_4(\text{P}_3\text{O}_9)_2$ . The kinetic of thermal dehydration of  $\text{CdK}_4(\text{P}_3\text{O}_9)_2 \cdot 2\text{H}_2\text{O}$  was studied using thermal analyses TGA-DTA coupled by two different methods. In this work, the kinetic and thermodynamic parameters for the dehydration process of  $\text{CdK}_4(\text{P}_3\text{O}_9)_2 \cdot 2\text{H}_2\text{O}$  are reported for the first time. It is to be noticed that  $\text{CdK}_4(\text{P}_3\text{O}_9)_2 \cdot 2\text{H}_2\text{O}$  and  $\text{CdK}_4(\text{P}_3\text{O}_9)_2$  are binary fertilizers type PK and can be used in the production of fertilizers.  $\text{CdK}_4$

$(\text{P}_3\text{O}_9)_2 \cdot 2\text{H}_2\text{O}$  and  $\text{CdK}_4(\text{P}_3\text{O}_9)_2$  are stable under the normal conditions of temperature and pressure.

## Experimental

### Chemical Preparation

Polycrystalline samples of the title compound were prepared by slowly adding dilute cyclotriphosphoric acid to an aqueous solution of manganese carbonate and potassium carbonate with a stoichiometric ratio  $\text{K/Mn} = 4$ , according to the following chemical reaction:

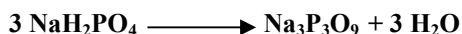


The solution obtained was then slowly evaporated at room temperature until polycrystalline samples of  $\text{CdK}_4(\text{P}_3\text{O}_9)_2 \cdot 2\text{H}_2\text{O}$  were obtained. The cyclotriphosphoric acid used in this reaction was prepared from an aqueous solution of  $\text{Na}_3\text{P}_3\text{O}_9$  passed through an ion-exchange resin "Amberlite IR 120" [6].  $\text{Na}_3\text{P}_3\text{O}_9$  was obtained by thermal [7] treatment of sodium

\*Corresponding author: **El Kababi K**

Laboratoire de Chimie-Physique des Matériaux, Faculté des Sciences Ben M'sik, B. P. 7955. Casablanca. Maroc

dihydrogenomonophosphate, at 530°C for 5 hours in air according to:



The weight loss performed by slowly heating up to a temperature of 200°C, confirms the compound as a dihydrate,  $\text{CdK}_4(\text{P}_3\text{O}_9)_2 \cdot 2\text{H}_2\text{O}$ .

$\text{CdK}_4(\text{P}_3\text{O}_9)_2$  was obtained by total dehydration of  $\text{CdK}_4(\text{P}_3\text{O}_9)_2 \cdot 2\text{H}_2\text{O}$  [3, 8, 9] under atmospheric pressure, between 350 and 420°C. With a further increase in temperature,  $\text{CdK}_4(\text{P}_3\text{O}_9)_2$  melts at 431°C.

Both cyclotriphosphates,  $\text{CdK}_4(\text{P}_3\text{O}_9)_2 \cdot 2\text{H}_2\text{O}$  and its anhydrous form  $\text{CdK}_4(\text{P}_3\text{O}_9)_2$ , described in the present work are stable for years in normal conditions of temperature and humidity.

$\text{CdK}_4(\text{P}_3\text{O}_9)_2 \cdot 2\text{H}_2\text{O}$  and  $\text{CdK}_4(\text{P}_3\text{O}_9)_2$  have been studied through different techniques with the experimental conditions described below.

### XRD, Crystal data, intensity data collection and structure

X-ray diffraction. Powder diffraction patterns were registered with a SIEMENS diffractometer type D 5000 using  $\text{CuK}\alpha 1$  radiation ( $\lambda = 1.5406\text{\AA}$ ).

Infrared spectrometry. Spectra were recorded in the range 4000-400  $\text{cm}^{-1}$  with a Perkin-Elmer IR 983G spectrophotometer, using samples dispersed in spectroscopically pure KBr pellets.

Thermal behavior. Thermal analyses TGA-DTA coupled were performed using the multimodule 92 Setaram Analyzer operating from room temperature up to 1400°C, in a platinum crucible, at various heating rates from 1 to 15°C/min. The differential scanning calorimetry (DSC) was performed with a Setaram DSC 92 apparatus.

### Crystallographic characterization

Crystal Data.  $\text{CdK}_4(\text{P}_3\text{O}_9)_2 \cdot 2\text{H}_2\text{O}$  is isotypic to  $\text{MnK}_4(\text{P}_3\text{O}_9)_2 \cdot 2\text{H}_2\text{O}$  whose atomic arrangement was determined by M. T. Averbuch-Pouchot [10].  $\text{CdK}_4(\text{P}_3\text{O}_9)_2 \cdot 2\text{H}_2\text{O}$  [8] is triclinic P-1 with the following unit-cell dimensions:  $a = 9.235(4)\text{\AA}$ ,  $b = 7.599(3)\text{\AA}$ ,  $c = 7.148(1)\text{\AA}$ ,  $\alpha = 96.38(2)^\circ$ ,  $\beta = 103.90(5)^\circ$ ,  $\gamma = 102.06(3)^\circ$  and  $Z = 1$ .

$\text{CdK}_4(\text{P}_3\text{O}_9)_2$  is isotypic to a series of five cyclotriphosphates corresponding to the general formula  $\text{M}^{\text{II}}\text{Ti}_4(\text{P}_3\text{O}_9)_2$  ( $\text{M}^{\text{II}} = \text{Mg}^{2+}$ ,  $\text{Co}^{2+}$ ,  $\text{Zn}^{2+}$ ,  $\text{Cd}^{2+}$ ,  $\text{Ca}^{2+}$ ) [11], of  $\text{MnTi}_4(\text{P}_3\text{O}_9)_2$  [8], of  $\text{MnCa}_2(\text{P}_3\text{O}_9)_2$  [12,13,14] and also of  $\text{MnK}_4(\text{P}_3\text{O}_9)_2$  studied in our laboratory. It is worth noting that  $\text{CdK}_4(\text{P}_3\text{O}_9)_2 \cdot 2\text{H}_2\text{O}$  [8,9] has never been studied except its crystallographic characterization.

$\text{CdK}_4(\text{P}_3\text{O}_9)_2$  crystallizes in the rhombohedral system, space group P-3<sub>1</sub>c,  $Z = 2$  with the following unit-cell dimensions:  $a = b = 7.337(3)\text{\AA}$  and  $c = 19.920(1)\text{\AA}$ . The X-ray diffractogram of  $\text{CdK}_4(\text{P}_3\text{O}_9)_2$  is reported in Figure 1. Indexing of the X-ray diffraction pattern of  $\text{CdK}_4(\text{P}_3\text{O}_9)_2$  is reported in Table 1.

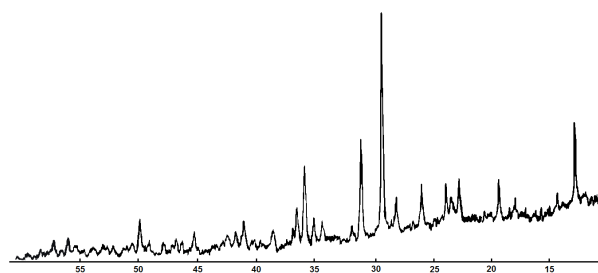


Figure 1 X-ray powder diffractograms of the phosphate  $\text{CdK}_4(\text{P}_3\text{O}_9)_2 \cdot 2\text{H}_2\text{O}$ .

Table 1 Powder diffraction data of  $\text{CdK}_4(\text{P}_3\text{O}_9)_2$

hkl	d <sub>cal</sub> (Å)	d <sub>obs</sub> (Å)	100I/I <sub>0</sub>	hkl	d <sub>cal</sub> (Å)	d <sub>obs</sub> (Å)	100I/I <sub>0</sub>
-	-	8.17	26	013	4.62	4.57	32
-	-	7.48	27	014	3.933	3.912	32
-	-	6.94	56	-	-	3.798	26
010	6.40	6.44	23	110	3.700	3.713	32
011	6.10	6.18	27	111	3.634	3.625	17
-	-	5.66	21	112	3.465	3.434	31
012	5.40	5.48	20	006	3.331	3.332	18
-	-	5.22	21	021	3.164	3.186	26
004	5.00	4.95	26	114	2.978	3.036	100
-	-	4.80	21	023	2.887	2.876	50

Theta range: 6-30°, Step size: 0.02°(2θ), Counting time : 30s

### Infrared study

The IR absorption spectrum of  $\text{CdK}_4(\text{P}_3\text{O}_9)_2 \cdot 2\text{H}_2\text{O}$  is reported in Figure 2a and shows in the domain, 4000-3000  $\text{cm}^{-1}$ , characteristic of the valence vibration bands ( $\nu$  O-H), a large and strong band at 3450  $\text{cm}^{-1}$  due to hydrogen bonds [15]. The domain, 1700-1600  $\text{cm}^{-1}$ , characteristic of the bending vibration bands of water ( $\delta$  HOH), shows one band at 1630  $\text{cm}^{-1}$  suggesting the existence of one type of water molecules in accordance with the crystalline structure of  $\text{CdK}_4(\text{P}_3\text{O}_9)_2 \cdot 2\text{H}_2\text{O}$ , resolved on the basis of its isotopic compound  $\text{MnK}_4(\text{P}_3\text{O}_9)_2 \cdot 2\text{H}_2\text{O}$ .

The range 1400-650  $\text{cm}^{-1}$ , characteristic of the valence vibration bands of the cycle [16,17], as well as possible bands due to interactions between  $\text{P}_3\text{O}_9$  cycles and water molecules and also water vibration modes will be examined on the basis, of the crystalline structure of  $\text{CdK}_4(\text{P}_3\text{O}_9)_2 \cdot 2\text{H}_2\text{O}$  isotypic to  $\text{MnK}_4(\text{P}_3\text{O}_9)_2 \cdot 2\text{H}_2\text{O}$ , and of our results of the 30 normal calculated frequencies of the  $\text{P}_3\text{O}_9$  ring with high symmetry  $D_{3h}$ , of the frequency shifts during theoretical and successive isotopic substitutions of the equivalent atoms  $^{31}\text{P}$ - $^{33}\text{P}$ ,  $^{16}\text{O}_i$ - $^{18}\text{O}_i$  and  $^{16}\text{O}_e$ - $^{18}\text{O}_e$ , of the three equivalent atoms ( $3\text{P}$ ,  $3\text{O}_i$  and  $6\text{O}_e$ ) belonging to the  $\text{P}_3\text{O}_i\text{O}_e$  ring ( $D_{3h}$ ).  $\text{CdK}_4(\text{P}_3\text{O}_9)_2 \cdot 2\text{H}_2\text{O}$  crystallizes in the triclinic system, space group P-1 (Ci), with a unit-cell containing two cycles  $\text{P}_3\text{O}_9$  (one cycle is deduced from the other by the center of symmetry) with no local symmetry  $C_1$ . The reduced representation of the internal modes of the isolated ring  $\text{P}_3\text{O}_9$  with  $D_{3h}$  symmetry is:

$$\Gamma_{\text{int}} = 4A'_1(-, \text{Ra}) + 2A'_2(-, -) + 6E'(\text{IR}, \text{Ra}) + A''_1(-, -) + 3A''_2(\text{IR}, -) + 4E''(-, \text{Ra}).$$

The cycle  $\text{P}_3\text{O}_9$  is built, theoretically, by three external ( $\text{PO}_2$ ) groups and the  $\text{P}_3\text{O}_i$  ring. Theoretical group analysis leads, for the valence vibration bands (the only ones which we consider here) to  $\Gamma_{\text{PO}_2} = A'_1(-, \text{Ra}) + A''_2(\text{IR}, -) + E'(\text{IR}, \text{Ra}) + E''(-, \text{Ra})$  and  $\Gamma_{\text{P}_3\text{O}_i} = A'_1(-, \text{Ra}) + A'_2(-, -) + 2E'(\text{IR}, \text{Ra})$ . Theoretical

group analysis predicts six valence vibration bands for the  $\text{PO}_2$  groups, six valence vibration bands for the  $\text{P}_3\text{O}_9$  ring and 18 bending vibration bands for the  $\text{P}_3\text{O}_9$  ring,  $\Gamma_{\text{bending}} = 2A'_1(\text{Ra}) + A'_2(-,-) + A''_1(-,-) + 2A''_2(\text{IR},-) + 3E'(\text{IR}, \text{Ra}) + 3E''(-,\text{Ra})$ . These thirty fundamental frequencies of the cycle,  $D_{3h}$ , were calculated, by the MNDO method [28], and their attribution was made by using successive isotopic substitutions  $^{16}\text{Oi}$ - $^{18}\text{Oe}$ ,  $^{31}\text{P}$ - $^{33}\text{P}$  and  $^{16}\text{Oe}$ - $^{18}\text{Oe}$  (Table 2). From the isotopic effects ( $\Delta\nu$ ), the contribution of each group of atoms,  $\text{POiP}$  and/or  $\text{PO}_2$ , to each calculated normal frequency was determined. With this intention, we supposed that the pure movements of the  $\text{POiP}$  groups must leave the external oxygen atoms,  $\text{Oe}$ , fixed and those due to 100% of internal groups,  $\text{Oi}$ , fixed. By means of this assumption, the percentage of participation of each group was determined (Table 2). The IR spectrum of  $\text{CdK}_4(\text{P}_3\text{O}_9)_2 \cdot 2\text{H}_2\text{O}$  shows, in plus, 7, valence fundamental frequencies (in the range  $1400\text{--}650\text{ cm}^{-1}$ ). This number is less than, 12, predicted as well as for the isolated cycle with symmetry  $C_1$  and for the crystalline unit-cell with group factor  $C_1$  in  $\text{CdK}_4(\text{P}_3\text{O}_9)_2 \cdot 2\text{H}_2\text{O}$  containing two  $\text{P}_3\text{O}_9$  cycles,  $\Gamma_{\text{val}} = 12\text{Au}(\text{IR},-) + 12\text{Ag}(-,\text{Ra})$ . In fact, during the passage from the isolated cycle, with symmetry  $C_1$ , to the crystalline unit-cell, each mode A of the site group is resolved into  $\text{Au}(\text{IR},-) + \text{Ag}(-,\text{Ra})$ . It seems that the vibrational couplings between the two  $\text{P}_3\text{O}_9$  cycles of the unit-cell, are absent or very weak, and don't disturb the IR spectrum of the title compound and don't allow the increasing of the IR frequencies to compare with those predicted for an isolated cycle with symmetry  $C_1$ .

We notice that the calculated frequencies values for the  $D_{3h}$  symmetry, are similar to those observed in the IR spectrum of  $\text{CdK}_4(\text{P}_3\text{O}_9)_2 \cdot 2\text{H}_2\text{O}$ . On the basis of our results of calculations, using the MNDO method [28], the fundamental frequencies of the  $\text{P}_3\text{O}_9^{3-}$  cycle with high symmetry  $D_{3h}$  and the correlation group  $D_{3h}$  – group with low symmetry  $C_1$ , the attribution of the valence frequencies of the cycle, is proposed in table 3.

The crystalline structure of  $\text{MgTi}_4(\text{P}_3\text{O}_9)_2$  [11], proposed for  $\text{CdK}_4(\text{P}_3\text{O}_9)_2$  new phase, is described in the space group  $P\text{-}3_1c$  ( $D_{3d}^2$ ) with two formula units ( $Z = 2$ ) per unit-cell. The crystalline unit-cell contains four cycles occupying sites with local symmetry  $C_3$ . During the passage from the symmetry  $D_{3h}$  to the  $C_3$  symmetry of the cycle, supposed isolated, of  $\text{CdK}_4(\text{P}_3\text{O}_9)_2$ , the simple normal modes  $A'_1$ ,  $A'_2$ ,  $A''_1$  and  $A''_2$ , Of the symmetry  $D_{3h}$ , are resolved each one into the mode A, of the symmetry  $C_3$ , and the doubly degenerate  $E'$  and  $E''$  modes are resolved into the mode E of the symmetry  $C_3$ . For this reason, 7 IR bands are predicted, in the range of valence vibrations, for the isolated cycle with symmetry  $C_3$  which has four vibration frequencies with simple modes A and four modes E. The experimental IR spectrum of  $\text{CdK}_4(\text{P}_3\text{O}_9)_2$  (Figure 2b) shows, in the domain  $1400\text{--}650\text{ cm}^{-1}$ , 7 IR fundamental bands. This number of six bands is less than that predicted for an isolated cycle with symmetry  $C_3$ . When we pass from the isolated cycle with symmetry  $C_3$  to the crystalline unit-cell of  $\text{CdK}_4(\text{P}_3\text{O}_9)_2$  containing 4 cycles in interaction between them, the four IR bands with modes E, of the  $C_3$  symmetry, should appear in the shape of a doublet of frequencies with modes Eu of the group factor  $D_{3d}$ .

**Table2** IR frequencies and displacements ( $\Delta\nu$  in  $\text{cm}^{-1}$ ) calculated for the  $D_{3h}$  symmetry and for the substitutions of the internal oxygen atoms (Oi), of the external oxygen atoms (Oe) by the isotope  $^{18}\text{O}$  and of the phosphorus atoms by the isotope  $^{33}\text{P}$  and percentage of participation of the POP and  $\text{PO}_2$  groups

$^{31}\text{P}_3^{16}\text{O}_9^{3-}$	$^{31}\text{P}_3^{18}\text{O}_9^{3-}$	$^{33}\text{P}_3^{16}\text{O}_9^{3-}$	$^{33}\text{P}_3^{18}\text{O}_9^{3-}$	$^{31}\text{P}_3^{16}\text{O}_9^{3-}$	$^{31}\text{P}_3^{18}\text{O}_9^{3-}$	$^{33}\text{P}_3^{16}\text{O}_9^{3-}$	$^{33}\text{P}_3^{18}\text{O}_9^{3-}$	% of
$\nu(\text{cm}^{-1})$	$\nu(\text{cm}^{-1})$	$\Delta\nu(\text{cm}^{-1})$	$\nu(\text{cm}^{-1})$	$\Delta\nu(\text{cm}^{-1})$	$\nu(\text{cm}^{-1})$	$\Delta\nu(\text{cm}^{-1})$	$\nu(\text{cm}^{-1})$	Participation
1288.39	1287.80	0.59	1269.56	18.83	1249.94	38.45	1249.94	$\nu_{\text{as}}\text{PO}_2$ [99]
1272.42	1272.03	0.39	1254.33	18.09	1233.29	39.13	1233.29	{ $\nu_{\text{as}}\text{PO}_2$ [100]
1272.42	1272.03	0.39	1254.33	18.09	1233.29	39.13	1233.29	
1225.23	1179.02	46.20	1215.36	9.87	1223.90	1.32	1223.90	{ $\nu_{\text{as}}\text{POP}$ [98] + $\nu_{\text{as}}\text{PO}_2$ [2]
1225.23	1179.02	46.20	1215.36	9.87	1223.90	1.32	1223.90	
1169.25	1168.86	0.39	1156.27	12.98	1127.60	41.65	1127.60	$\nu_{\text{as}}\text{PO}_2$ [100]
1108.62	1098.55	10.07	1102.24	6.38	1062.88	45.74	1062.88	{ $\nu_{\text{as}}\text{POP}$ [18] + $\nu_{\text{as}}\text{PO}_2$ [82]
1108.62	1098.55	10.07	1102.24	6.38	1062.88	45.74	1062.88	
1059.41	1010.98	48.43	1053.00	6.41	1058.95	0.46	1058.95	$\nu_{\text{as}}\text{POP}$ [100]
780.72	768.35	12.36	765.35	15.37	775.94	4.78	775.94	{ $\nu_{\text{as}}\text{POP}$ [73] + $\delta\text{PO}_2$ [27]
780.72	768.35	12.36	765.35	15.37	775.94	4.78	775.94	
671.06	659.43	11.64	663.25	7.82	660.26	10.81	660.26	$\nu_{\text{as}}\text{POP}$ [52] + $\delta\text{PO}_2$ [48]
559.30	537.04	22.26	555.32	3.98	552.99	6.31	552.99	{ $\delta\text{POP}$ (8cycle) [78] + $\delta\text{PO}_2$ [22]
511.49	496.11	15.38	509.22	2.27	501.42	10.07	501.42	
436.79	433.11	3.68	432.47	4.32	422.93	13.86	422.93	{ $\delta\text{POP}$ [21] + $\delta\text{PO}_2$ [79]
436.79	433.11	3.68	432.47	4.32	422.93	13.86	422.93	
420.11	417.43	2.68	416.98	3.13	411.08	9.03	411.08	$\gamma_{\text{as}}\text{PO}_2$ [78]
418.64	406.27	12.37	416.98	1.66	410.11	8.52	410.11	{ $\gamma_{\text{POP}}$ [59] + $\gamma_{\text{T}}\text{PO}_2$ [41]
418.64	406.27	12.37	416.98	1.66	410.11	8.52	410.11	
302.05	301.64	0.41	301.40	0.64	289.37	12.68	289.37	$\delta\text{PO}_2$ [98]
298.72	292.60	6.12	298.18	0.54	289.37	9.35	289.37	{ $\delta\text{POP}$ [40] + $\gamma_{\text{W}}\text{PO}_2$ [60]
298.72	292.60	6.12	298.18	0.54	289.37	9.35	289.37	
280.98	279.09	1.89	279.07	1.91	269.75	11.23	269.75	{ $\gamma_{\text{POP}}$ [14] + $\gamma_{\text{T}}\text{PO}_2$ [86]
280.98	279.09	1.89	279.07	1.91	269.75	11.23	269.75	
256.58	253.04	3.55	255.07	1.51	246.51	10.07	246.51	{ $\delta\text{POP}$ [26] + $\gamma_{\text{W}}\text{PO}_2$ [74]
256.58	253.04	3.55	255.07	1.51	246.51	10.07	246.51	
214.09	214.06	0.03	214.06	0.03	201.82	12.28	201.82	$\gamma_{\text{T}}\text{PO}_2$ [100]
49.31	48.52	0.79	49.29	0.02	47.21	2.10	47.21	$\gamma_{\text{POP}}$ [27] + $\gamma_{\text{R}}\text{PO}_2$ [73]
35.02	34.37	0.65	35.02	0.00	33.59	1.43	33.59	{ $\gamma_{\text{POP}}$ [33] + $\gamma_{\text{R}}\text{PO}_2$ [67]
35.02	34.37	0.65	35.02	0.00	33.59	1.43	33.59	

$\nu_{\text{as}}$  : asymmetric stretching;  $\nu_{\text{s}}$  : symmetric stretching;  $\delta$  : bending;  $\gamma$  : out of plane  $\text{P}_3\text{O}_9$ ;

$\gamma_{\text{W}}$  : wagging ( $\gamma_{\perp}\text{PO}_2$ );  $\gamma_{\text{R}}$  : rocking ( $\gamma_{\parallel}\text{PO}_2$ );  $\gamma_{\text{T}}$  : twisting; Oi : internal oxygen atom of the ring and Oe: external oxygen atom of the ring



**Table 3** comparison of valence vibratory modes of the cycle, free with molecular group  $\text{D}_{3h}$  ( $\nu$  calculated), with site symmetry  $\text{C}_1$  and of the two cycles of the unit-cell in interaction between them in  $\text{CdK}_4(\text{P}_3\text{O}_9)_2 \cdot 2\text{H}_2\text{O}$

Molecular group D <sub>3h</sub>				Site symmetry C <sub>1</sub>		Group factor C <sub>i</sub>	
ν <sub>cal</sub> (cm <sup>-1</sup> )	I (Km/mol)	vibration	Mode Activity	Mode Activity	Mode Activity	CdK <sub>4</sub> (P <sub>3</sub> O <sub>9</sub> ) <sub>2</sub> ·2H <sub>2</sub> O	
1288	4264	ν <sub>as</sub> PO <sub>2</sub>	A'' <sub>2</sub> (IR, -)	→ A (IR,Ra)	↘ Ag (-,Ra) ↗ Au (IR,-)	1284 (VS)	
{1272 1272}	{0 0}	ν <sub>as</sub> PO <sub>2</sub>	E'' (-, Ra)	↘ A (IR,Ra)	↘ Ag (-,Ra) ↗ Au (IR,-)		
				↗ A (IR,Ra)	↗ Ag (-,Ra) ↘ Au (IR,-)		
{1225 1225}	{7713 7714}	ν <sub>as</sub> POP	E' (IR,Ra)	↘ A (IR,Ra)	↘ Ag (-,Ra) ↗ Au (IR,-)		
				↗ A (IR,Ra)	↗ Ag (-,Ra) ↘ Au (IR,-)		
1169	0	ν <sub>s</sub> PO <sub>2</sub>	A' <sub>1</sub> (-, Ra)	→ A (IR,Ra)	↘ Ag (-,Ra) ↗ Au (IR,-)	1150 (m)	
{1108 1108}	{452 451}	ν <sub>s</sub> PO <sub>2</sub>	E' (IR,Ra)	↘ A (IR,Ra)	↘ Ag (-,Ra) ↗ Au (IR,-)		
				↗ A (IR,Ra)	↗ Ag (-,Ra) ↘ Au (IR,-)		
1059	0	ν <sub>as</sub> POP	A'' <sub>2</sub> (-, -)	→ A (IR,Ra)	↘ Ag (-,Ra) ↗ Au (IR,-)	1000 (VS)	
{781 781}	{1415 1414}	ν <sub>s</sub> POP	E' (IR,Ra)	↘ A (IR,Ra)	↘ Ag (-,Ra) ↗ Au (IR,-)		
				↗ A (IR,Ra)	↗ Ag (-,Ra) ↘ Au (IR,-)		
671	0	ν <sub>s</sub> POP	A' <sub>1</sub> (-, Ra)	→ A (IR,Ra)	↘ Ag (-,Ra) ↗ Au (IR,-)	684 (m)	

VS: very strong S: Strong m: medium sh: shoulder

**Table 4** Attribution of the observed valence IR frequencies ( $\text{cm}^{-1}$ ) of the  $\text{P}_3\text{O}_9$  ring ( $\text{C}_3$ ) in  $\text{CdK}_4(\text{P}_3\text{O}_9)_2 \cdot 2\text{H}_2\text{O}$  (I) and  $\text{CdK}_4(\text{P}_3\text{O}_9)_2$  (II)

S. G.			$\Delta\nu$ ( $\text{cm}^{-1}$ )			(I) (II)		Main Movement
$\text{C}_3$	$\nu_{\text{cal}}$	I/Imax	$^{16}\text{O}_i-^{18}\text{O}_i$	$^{31}\text{P}-^{33}\text{P}$	$^{16}\text{O}_e-^{18}\text{O}_e$	(I)	(II)	
	1288.39	55.20		0.59	18.83	38.45		$\nu_{\text{as}}\text{PO}_2$
	1272.42	0.01		0.39	18.09	39.13	1284	$\nu_{\text{as}}\text{PO}_2$
	1272.42	0.01		0.39	18.09	39.13	1280	$\nu_{\text{as}}\text{PO}_2$
	1225.23	100.00		46.20	9.87	1.32		$\nu_{\text{as}}\text{POP}$
	1225.23	100.00		46.20	9.87	1.32		$\nu_{\text{as}}\text{POP}$
	1169.25	0.00		0.39	12.98	41.65		$\nu_s\text{PO}_2$
	1108.62	5.81		10.07	6.38	45.74	1150	$\nu_s\text{PO}_2$
	1108.62	5.81		10.07	6.38	45.74	1095	$\nu_s\text{PO}_2$
	1059.41	0.00		48.43	6.41	0.46	1000	$\nu_{\text{as}}\text{POP}$
						858sh	1009	POP combination
						874sh	874sh	
	780.72	18.34		12.36	15.37	4.78	771	$\nu_s\text{POP}$
	780.72	18.34		12.36	15.37	4.78	747	$\nu_s\text{POP}$
	671.06	0.01		11.64	7.82	10.67	684	$\nu_s\text{POP}$
						684	684	$\nu_s\text{POP}$

$\Delta\nu$  ( $\text{cm}^{-1}$ ) : effect of the isotopic substitution;  $\Delta\nu$  ( $\text{cm}^{-1}$ ) : difference between the calculated Value of the frequency before and after the substitution; S. G. : site group.

This situation is due to the correlation group  $\text{C}_3$  – group factor  $\text{D}_{3d}$  resolving the mode A, of  $\text{C}_3$ , into modes  $\text{A}_{1g}(-, \text{Ra}) + \text{A}_{2g}(-, -) + \text{A}_{1u}(-, -) + \text{A}_{2u}(\text{IR}, \text{Ra})$ , of the group  $\text{D}_{3d}$ , and the mode E into  $2\text{Eg}(-, \text{Ra}) + 2\text{Eu}(\text{IR}, -)$ .

We notice that the calculated frequencies values of the  $\text{D}_{3h}$  symmetry are similar to those observed in the IR spectra of  $\text{CdK}_4(\text{P}_3\text{O}_9)_2 \cdot 2\text{H}_2\text{O}$  and its anhydrous form  $\text{CdK}_4(\text{P}_3\text{O}_9)_2$ . On the basis of our results of calculations of the normal frequencies of the  $\text{P}_3\text{O}_9^{3-}$  cycle with high symmetry  $\text{D}_{3h}$  and the

correlations group  $D_{3h}$  – groups with low symmetries  $C_3$  and  $C_1$ , the assignment of the valence frequencies of the cycle, is given in **table 4**.

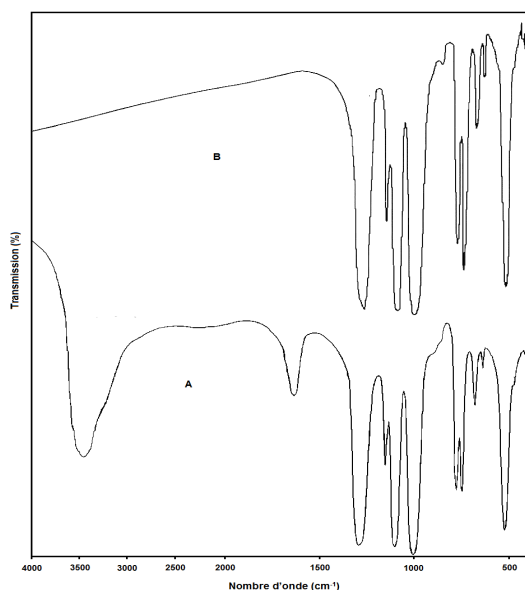


**Figure 2** IR spectra of the phosphates: (a)  $CdK_4(P_3O_9)_2 \cdot 2H_2O$  and (b)  $CdK_4(P_3O_9)_2$

### Thermal Behavior

The two curves corresponding to the TGA and DTA analyses in air atmosphere and at a heating rate  $3^\circ C/min$  of  $CdK_4(P_3O_9)_2 \cdot 2H_2O$  are shown in **Figure 3**. The loss of water of dehydration on the TG curve (**Figure 3**) takes place in three steps between  $50^\circ C$  and  $350^\circ C$  corresponding to 4.62% weight loss instead of 4.63% for the theoretical one assuming  $2H_2O$  in the formula.

The dehydration of the cyclotriphosphate dihydrate of cadmium and potassium  $CdK_4(P_3O_9)_2 \cdot 2H_2O$  happens in three steps in three temperature ranges  $50 - 135^\circ C$ ,  $135 - 215^\circ C$  and  $215 - 350^\circ C$  (**Figure 3**). In the thermogravimetric (TG) curve (**Figure 3**), the first stage between  $50$  and  $135^\circ C$  attributed to the elimination of 1.1 water molecules corresponding to 2.54 weight loss, the second stage from  $135$  to  $215^\circ C$  is due to the elimination of 0.6 water molecule corresponding to 1.39 weight loss and the third stage  $215 - 350^\circ C$  attributed to the elimination of 0.3 water molecule corresponding to 0.69 weight loss.

The thermal analysis curve (DTA in **Figure 3**) shows that the cyclotriphosphate  $CdK_4(P_3O_9)_2 \cdot 2H_2O$  undertakes at  $68^\circ C$  and  $217^\circ C$  two endothermic peaks and one exothermic peak at  $213^\circ C$ . The first endothermic peak at  $68^\circ C$  is due to the dehydration (departure of  $1H_2O$ ) of the title compound,  $CdK_4(P_3O_9)_2 \cdot 2H_2O$ , well confirmed by the weight loss observed on the TG curve (**Figure 3**) between  $50^\circ C$  and  $135^\circ C$ . The second endothermic peak at  $217^\circ C$  is due to the dehydration (departure of  $1H_2O$ ) of the title compound,  $CdK_4(P_3O_9)_2 \cdot 2H_2O$ , well confirmed by the weight loss observed on the TG curve (**Figure 3**) between  $135^\circ C$  and  $350^\circ C$ . The only exothermic peak at  $213^\circ C$  on the DTA curve (**Figure 3**) is due to the crystallization of the anhydrous cyclotriphosphate  $CdK_4(P_3O_9)_2$  well characterized by X-ray diffraction (**Figure 1**) and infrared spectrometry (**Figure 2b**).

The thermal behavior of  $CdK_4(P_3O_9)_2 \cdot 2H_2O$  was also studied in a step manner of temperature by X-ray diffraction and IR absorption experiments between  $20^\circ C$  and  $431^\circ C$ .  $CdK_4(P_3O_9)_2 \cdot 2H_2O$  is stable until  $50^\circ C$ . The removal of the two water molecules of hydration of  $CdK_4(P_3O_9)_2 \cdot 2H_2O$ , observed in the temperature range  $50-350^\circ C$ , neither destroys the crystalline network nor yields to an intermediate amorphous phase but leads to the crystallization of a new ring phosphate (**Figure 1**) which exhibits the IR absorption bands characteristic of a cyclic phosphate [16-27] (**Figure 2b**). The water characteristic vibrations have disappeared after the complete dehydration at  $350^\circ C$  (**Figure 2b**). The product of the total dehydration of  $CdK_4(P_3O_9)_2 \cdot 2H_2O$  between  $350$  and  $420^\circ C$  is a new anhydrous cyclotriphosphate  $CdK_4(P_3O_9)_2$  characterized in the present study. In fact, the only exothermic peak observed on the DTA curve (**Figure 3**) at  $213^\circ C$  corresponds to the crystallization of  $CdK_4(P_3O_9)_2$ . With further increase in temperature,  $CdK_4(P_3O_9)_2$  remains stable and melts at  $431^\circ C$ .

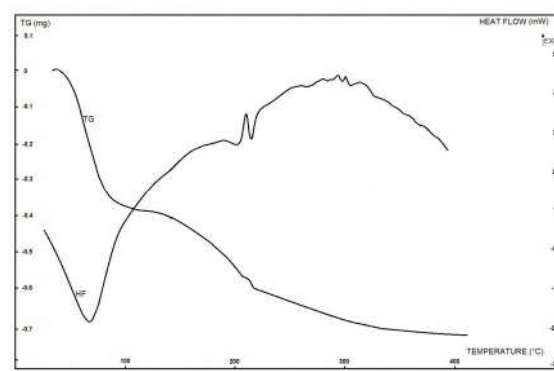


**Figure 3** TGA and DTA curves of  $CdK_4(P_3O_9)_2 \cdot 2H_2O$  at rising temperature ( $3^\circ C/min$ )

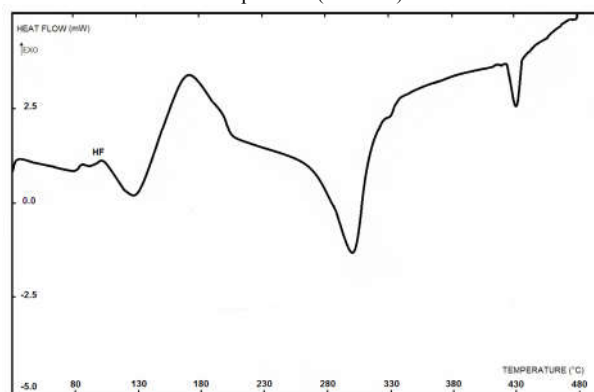


**Figure 4** DSC curve of  $CdK_4(P_3O_9)_2 \cdot 2H_2O$  at rising temperature ( $3^\circ C/min$ )

The curves of differential scanning calorimetry (DSC) at different rising temperatures ( $3$  and  $10^\circ C/min$ ) of  $CdK_4(P_3O_9)_2 \cdot 2H_2O$ , represented by the **Figures 4 and 5**, show one exothermic peak at  $174^\circ C$  for  $3^\circ C/min$  ( $184^\circ C$  for  $10^\circ C/min$ ) and three endothermic peaks at  $129^\circ C$ ,  $302^\circ C$  and  $431^\circ C$  for  $3^\circ C/min$  ( $138^\circ C$ ,  $326^\circ C$  and  $443^\circ C$  for  $10^\circ C/min$ ) (**Figures 4 and 5**). The first two endothermic peaks correspond to the dehydration of  $CdK_4(P_3O_9)_2 \cdot 2H_2O$  and are then due to the departure of water molecules (peaks at  $129^\circ C$  ( $1H_2O$ ) and  $302^\circ C$  ( $1H_2O$ ) for  $3^\circ C/min$ ;  $138^\circ C$  ( $1H_2O$ ) and  $326^\circ C$  ( $1H_2O$ ) for  $10^\circ C/min$ ). The exothermic peaks at  $174^\circ C$  for  $3^\circ C/min$  and  $184^\circ C$  for  $10^\circ C/min$  are due to the crystallization of the

anhydrous form of the title compound,  $\text{CdK}_4(\text{P}_3\text{O}_9)_2$ , well characterized by X-ray diffraction (**Figure 1**) and infrared spectrometry (**Figure 2b**). The crystallization of  $\text{CdK}_4(\text{P}_3\text{O}_9)_2$  was also observed on the DTA curve at  $3^\circ\text{C}/\text{min}$  by an exothermic peak at  $213^\circ\text{C}$  (**Figure 3**). The endothermic peaks at  $431^\circ\text{C}$  for  $3^\circ\text{C}/\text{min}$  and  $443^\circ\text{C}$  for  $10^\circ\text{C}/\text{min}$  are due to the melting of  $\text{CdK}_4(\text{P}_3\text{O}_9)_2$ . The values of the enthalpy variations of all the peaks, observed in the differential scanning calorimetry (DSC) curves at different rising temperatures (3 and  $10^\circ\text{C}/\text{min}$ ) of  $\text{CdK}_4(\text{P}_3\text{O}_9)_2 \cdot 2\text{H}_2\text{O}$ , are gathered in the **Table 5**.

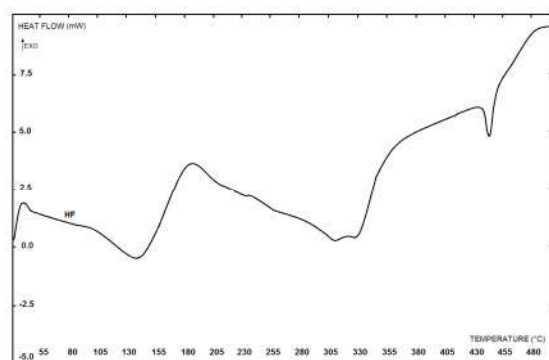


**Figure 5** DSC curve of  $\text{CdK}_4(\text{P}_3\text{O}_9)_2 \cdot 2\text{H}_2\text{O}$  at rising temperature ( $10^\circ\text{C}/\text{min}$ )

**Table 5** Enthalpy variations of all the peaks observed in the differential scanning calorimetry (DSC) curves at different rising temperatures (3 and  $10^\circ\text{C}/\text{min}$ ) of  $\text{CdK}_4(\text{P}_3\text{O}_9)_2 \cdot 2\text{H}_2\text{O}$

Peaks	$3^\circ\text{C}/\text{min}$		$10^\circ\text{C}/\text{min}$	
	T(°C)	$\Delta H$ (kcal.mol <sup>-1</sup> )	T(°C)	$\Delta H$ (kcal.mol <sup>-1</sup> )
First peak				
Removal of water (1H <sub>2</sub> O)	129	7.54	138	6.68
Second peak				
Crystallization of $\text{CdK}_4(\text{P}_3\text{O}_9)_2$	174	-7.72	184	-6.81
Third peak				
Removal of water (1H <sub>2</sub> O)	302	20.10	326	19.49
Fourth peak				
Melt of $\text{CdK}_4(\text{P}_3\text{O}_9)_2$	431	1.49 $\Delta S = 2.08$ cal. K <sup>-1</sup> . mol <sup>-1</sup>	443	1.28 $\Delta S = 1.82$ cal. K <sup>-1</sup> . mol <sup>-1</sup>

### Estimation of the thermodynamic functions

Various equations of kinetic analyses are known such as Kissinger's method[29], Kissinger-Akahira-Sunose (KAS) [30], Ozawa[31], Coats-Redfern[32] and Van Krevelen *et al.* [33] methods. Especially, the Ozawa and KAS equations were well described and widely used in the literature, therefore, these methods are selected in studying the kinetics of thermal dehydration of the title compound. So, water loss kinetic parameters were evaluated using the Kissinger-Akahira-Sunose (KAS) [30] and Ozawa[31] methods, from the curves  $\ln(v/T_m) = f(1/T_m)$  and  $\ln(v) = f(1/T_m)$  (**Figures 6 and 7**), where  $v$  is the heating rate and  $T_m$  the sample temperature at the thermal effect maximum. The characteristic temperatures at maximum dehydration rates,  $T_m$  in  $^\circ\text{C}$ , at different heating rates from the DTA curves of  $\text{CdK}_4(\text{P}_3\text{O}_9)_2 \cdot 2\text{H}_2\text{O}$  are gathered in **table 6**.

**Table 6** Characteristic temperatures at maximum dehydration rates,  $T_m$  in K, at different heating rates from the DTA curves of  $\text{CdK}_4(\text{P}_3\text{O}_9)_2 \cdot 2\text{H}_2\text{O}$

Heating rate $v$	$3^\circ\text{C}/\text{min}$	$5^\circ\text{C}/\text{min}$	$10^\circ\text{C}/\text{min}$	$15^\circ\text{C}/\text{min}$
First peak				
1H <sub>2</sub> O	68	75	81	88
second peak				
1H <sub>2</sub> O	217	225	230	238

From these temperatures and according to the Kissinger-Akahira-Sunose (KAS) [30] and Ozawa[31] methods, the apparent activation energies of dehydration were calculated for the cyclotriphosphate  $\text{CdK}_4(\text{P}_3\text{O}_9)_2 \cdot 2\text{H}_2\text{O}$ . For the Kissinger-Akahira-Sunose (KAS) [30] method, the slope of the resulting straight line of the curve:  $\ln(v/T_m^2) = f(1/T_m)$  (**Figure 6**), equals to :  $-E_a/R$ , allows the apparent activation energy to be calculated (**table 7**). Concerning the Ozawa[31] method, the slope of the resulting straight line on the curve :  $\ln(v) = f(1/T_m)$  (**Figure 7**), equals to  $-1.0516E/R$ , allows also the apparent activation energy to be calculated by this second way (**table 7**). The equations used for the two methods are the following:

$$\ln\left(\frac{v}{T_m^2}\right) = \ln\left(\frac{AR}{E}\right) - \left(\frac{E}{R}\right)\left(\frac{1}{T_m}\right) \quad \text{for KAS [30]} \quad (1)$$

$$\ln(v) = \ln\left(\frac{AR}{1.0516E}\right) - 1.0516\left(\frac{E}{R}\right)\left(\frac{1}{T_m}\right) \quad \text{for OZAWA [31]} \quad (2)$$

The pre-exponential factor or Arrhenius constant (A) can be calculated from both KAS[30] and Ozawa[31] methods. The related thermodynamic functions can be calculated by using the activated complex theory (transition state) of Eyring [34-36]. The following general equation can be written [36]:

$$A = \left(\frac{e\chi k_B T_m}{h}\right) \exp\left(\frac{\Delta S^*}{R}\right) \quad (3)$$

where  $e$  is the Neper number ( $e = 2.7183$ ),  $\chi$  is the transition factor, which is unity for the monomolecular reaction,  $k_B$  is the Boltzmann constant ( $k_B = 1.3806 \times 10^{-23} \text{ J K}^{-1}$ ),  $h$  is Plank's constant ( $h = 6.6261 \times 10^{-34} \text{ J s}$ ),  $T_m$  is the peak temperature of the DTA curve,  $R$  is the gas constant ( $R = 8.314 \text{ J K}^{-1} \text{ mol}^{-1}$ ) and  $\Delta S^*$  is the entropy change of transition state complex or entropy of activation. Thus, the entropy of activation may be calculated as follows:

$$\Delta S^* = R \ln \frac{Ah}{e\chi k_B T_m} \quad (4)$$

The enthalpy change of transition state complex or heat of activation ( $\Delta H^*$ ) and Gibbs free energy of activation ( $\Delta G^*$ ) of decomposition were calculated according to Eqs. (5) and (6), respectively:

$$\Delta H^* = E^* - R T_m \quad (5)$$

$$\Delta G^* = \Delta H^* - T_m \Delta S^* \quad (6)$$

Where,  $E^*$  is the activation energy  $E_a$  of both KAS[30] and Ozawa[31] methods. The values of the activation energy are gathered in **Table 7**. Thermodynamic functions were calculated from Eqs. (4), (5) and (6) and summarized in **Table 8**. The negative values of  $\Delta S^*$  from two methods for the dehydration step reveals that the activated state is less disordered compared to the initial state. These  $\Delta S^*$  values suggest a large number of degrees of freedom due to rotation which may be interpreted as

a « slow » stage/[36-38] in this step. The positive values of  $\Delta G^*$  at all studied methods are due to the fact that, the dehydration processes are not spontaneous. The positivity of  $\Delta G^*$  is controlled by a small activation entropy and a large positive activation enthalpy according to the Eq. 6. The endothermic peaks in DTA data agree well with the positive sign of the activation enthalpy ( $\Delta H^*$ ). The estimated thermodynamic functions  $\Delta S^*$  and  $\Delta G^*$  (Table 8) from two methods are different to some extent due to the different pre-exponential factor of about  $10^7$ . While  $\Delta H^*$  (Table 8) exhibits an independent behavior on the pre-exponential factor as seen from exhibiting nearly the same value.

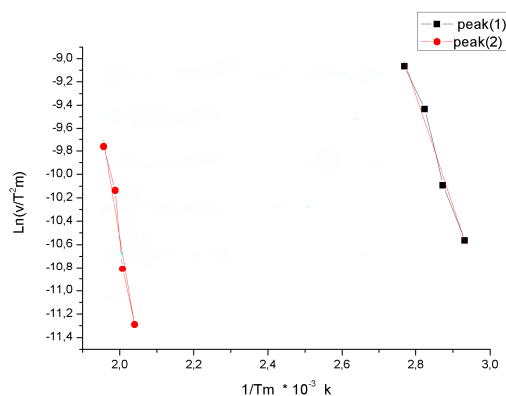


Figure 6  $\ln(v/Tm^2) = f(1/Tm)$  for  $CdK_4(P_3O_9)_2 \cdot 2H_2O$

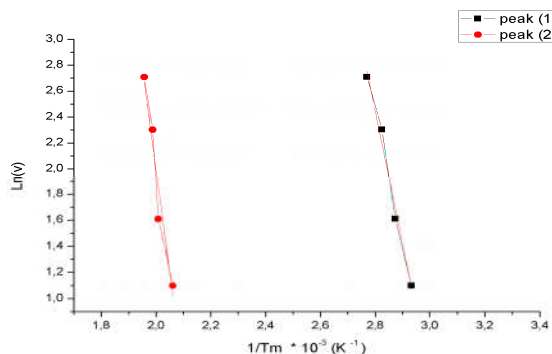


Figure 7  $\ln(v) = f(1/Tm)$  for  $CdK_4(P_3O_9)_2 \cdot 2H_2O$

**Table 7** Activation energy values  $E_a$ , pre-exponential factor (A) and correlation coefficient ( $r^2$ ) calculated by ozawa and KAS methods for the dehydration of  $CdK_4(P_3O_9)_2 \cdot 2H_2O$  under atmospheric pressure

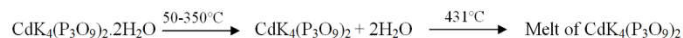
	Ozawa Method			KAS Method		
	$E_a / kJ. mol^{-1}$	$r^2$	$A / min^{-1}$	$E_a / kJ. mol^{-1}$	$r^2$	$A / min^{-1}$
First peak 1H <sub>2</sub> O	81.157	0.979	$2.210 \times 10^{12}$	79.605	0.9763	$8.109 \times 10^{11}$
Second peak 1H <sub>2</sub> O	124.664	0.943	$1.291 \times 10^{13}$	122.832	0.953	$2.9336 \times 10^{12}$

**Table 8** Values of  $\Delta S^\ddagger$ ,  $\Delta H^\ddagger$  and  $\Delta G^\ddagger$  for dehydration step of  $CdK_4(P_3O_9)_2 \cdot 2H_2O$  calculated according to ozawa and KAS equations

Model	$CdK_4(P_3O_9)_2 \cdot 2H_2O$					
	Ozawa method			KAS method		
	$\Delta S^\ddagger$ (J. K <sup>-1</sup> .mol <sup>-1</sup> )	$\Delta H^\ddagger$ (kJ.mol <sup>-1</sup> )	$\Delta G^\ddagger$ (kJ.mol <sup>-1</sup> )	$\Delta S^\ddagger$ (J. K <sup>-1</sup> .mol <sup>-1</sup> )	$\Delta H^\ddagger$ (kJ.mol <sup>-1</sup> )	$\Delta G^\ddagger$ (kJ.mol <sup>-1</sup> )
First peak 1H <sub>2</sub> O	-18.4964	78.156	84.833	-33.1106	76.604	88.557
Second peak 1H <sub>2</sub> O	-6.70611	120.415	123.842	-19.0310	118.584	128.309

## CONCLUSION

The present work concerns the thermal behavior of  $CdK_4(P_3O_9)_2 \cdot 2H_2O$ . This study allows us the identification and the characterization of a new phase  $CdK_4(P_3O_9)_2$ . The later is the final product of dehydration of  $CdK_4(P_3O_9)_2 \cdot 2H_2O$ . This anhydrous phase is stable until its melting point at 431°C. According to the known crystalline structure of  $CdK_4(P_3O_9)_2 \cdot 2H_2O$ , isotopic to  $MnK_4(P_3O_9)_2 \cdot 2H_2O$ , whose water molecules are of constitution and of one type remove the solid in three kinetic steps with an activation energy of dehydration calculated by Ozawa and KAS methods. The passage from the dihydrated phase,  $CdK_4(P_3O_9)_2 \cdot 2H_2O$ , to the anhydrous one,  $CdK_4(P_3O_9)_2$ , occurs with no amorphous phase and with no breaking of the cycle  $P_3O_9^{3-}$  and is accompanied with an enthalpy variation measured of 56.32 kJ. mol<sup>-1</sup> in the differential scanning calorimetry DSC. Two different methods Ozawa and KAS have been selected in studying the kinetics of thermal behavior of the title compound. In fact, in this work, the kinetics and thermodynamic parameters for the dehydration process of  $CdK_4(P_3O_9)_2 \cdot 2H_2O$  have been calculated and reported for the first time. Finally, we have examined and interpreted the IR spectra of the title compound and its anhydrous form  $CdK_4(P_3O_9)_2$  in the light of the crystalline structures of their isotopic compounds respectively, of our results of calculations of the IR fundamental frequencies of the cycle  $P_3O_9^{3-}$  with high symmetry  $D_{3h}$  and the successive isotopic substitutions of the equivalent atoms <sup>31</sup>P-<sup>33</sup>P, <sup>16</sup>O<sub>i</sub>-<sup>18</sup>O<sub>i</sub> and <sup>16</sup>O<sub>e</sub>-<sup>18</sup>O<sub>e</sub>, of the three equivalent atoms (3P, 3O<sub>i</sub> and 6O<sub>e</sub>) belonging to the  $P_3O_9$  ring. The thermal behavior of  $CdK_4(P_3O_9)_2 \cdot 2H_2O$  can be summarized by the following schema:



## References

1. K. Sbai, S. Belaaouad and K. Brouzi, Phosphorus, Sulfur, and Silicon, 177(5), 1085 (2002).
2. S. Belaaouad and K. Sbai, Powd. Diff., 17(1), 23 (2002).
3. S. Belaaouad, Thèse d'Etat. Faculté des Sciences Ben M'sik. Université Hassan II - Mohammedia. Casablanca. Maroc. (2002).
4. K. Sbai, A. Atibi et K. El Kababi, Thermochemica Acta, 389, 153 (2002).
5. EL. M. Tace, A. Charaf, I. Fahim, M. Moutaabbid, A. Kheireddine. F-E. Ouaalla, M. Tridane, K. Sbai, M. Radid and S. Belaaouad. Phosphorus, Sulfur, and Silicon and the Related Elements. 186: 7, 1501-1514. 7 Supplemental Materials. (2011).
6. A. Jouini and A. Durif, C. R. Acad. Sci., 297 (II), 573 (1983).
7. H. M. ONDIK, Acta Crystallogr., 18, 226 (1965).
8. M. T. Averbuch-Pouchot, J. L. Prisset and A. Durif, Eur. J. Solid State Inorg. Chem., 30, 71 (1993).
9. M. Belhabra, A. Kheireddine, H. Moutaabbid, B. Baptiste, R. Lamsatfi, I. Fahim, M. Tridane, M. Moutaabbid, S. Belaaouad. *International Journal of Recent Scientific Research*. Vol. 6, Issue, 12, 7832-7836, (2015).
10. M. T. Averbuch-Pouchot, Acta Crystallogr., Sect. B34, 20 (1978).



11. M. Tridane, I. Fahim, S. Benmokhtar and S. Belaaouad. Phosphorus Research Bulletin, Vol. 30, 1-7 (2015).
12. M. Tridane and S. Belaaouad. J. Mater. Environ. Sci. 6 (12) 3476-3482 (2015).
13. M. Tridane. Habilitation Universitaire. Faculté des Sciences Ben M'sik. Université Hassan II de Casablanca. Maroc. (2016).
14. M. Tridane, S. Belaaouad and K. Sbai, Solid State Sciences, 2, 701 (2000).
15. P. A. Kollman and C. L. Aller, Chem. Rev., 72, 283 (1972).
16. K. El Kababi., Thèse de Doctorat. Casablanca. Maroc. (2000).
17. K. El Kababi, K. Sbai and S. Vilminot, C. R. Acad. Sci., Série IIC. 3, 693 (2000).
18. M. H. Simonot-Grange, J. Solid State. Chem., 46, 76 (1983).
19. W. Bues and H. W. Gehrke, Z. Anorg. Allg. Chem., 288, 301 (1956).
20. N. Lazarev, Opt. Spect., 12, 60 (1962).
21. K. Sbai, Thèse d'Etat. Dijon. France. (1984).
22. P. Tarte, A. Rulmont, K. Sbai and M. H. Simonot-Grange, Spectrochim. Acta, 43A (3), 337 (1987).
23. K. Sbai, A. Abouimrane, A. Lahmidi, K. El Kababi, M. Hliwa and S. Vilminot, Ann. Chim. Sci. Mater., 25-suppl. 1, 139 (1999).
24. A. Abouimrane., Thèse de Doctorat. Casablanca. Maroc. (2000).
25. A. Abouimrane, K. Sbai, K. El Kababi, A. Lahmidi, A. Atibi et S. Vilminot, Phosphorus, Sulfur and Silicon, 179, 69 (2001).
26. K. Sbai, A. Abouimrane, K. El Kababi et S. Vilminot, J. Ther. Anal. Cal., 68, 109 (2002).
27. K. Sbai, A. Atibi, A. Charaf, M. Radid et A. Jouini, Ann. Chim. Sci. Mat., 26(6), 45 (2001).
28. M. J. S. Dewar and W. Thiel, J. Am. Chem. Soc., 99, 4899 (1977).
29. H. E. Kissinger, Anal. Chem., 29, 1702 (1957).
30. T. Akihira, T. Sunose, Trans. 1969 ; Res Report Chiba Inst. Technol. (Sci. Technol.), 16, 22 (1971).
31. T. A. Ozawa, Bull. Chem. Soc. Jpn., 38, 1881 (1965).
32. A. W. Coats, J. P. Redfern, Nature G, 20, 68 (1964).
33. D. W. Van Krevelins, P.J. Hoftijzer, Trans. I. Chem. E., 32, 5360 (1954).
34. D. Young, Decomposition of Solids, Academia Prague, (1984).
35. J. Rooney, J. Eyring, J. Mol. Catal. A. Chemical., L1, 96 (1995).
36. B. Boonchom, J. Chem. Eng. Data., 53, 1533 (2008).
37. L. Valaev, N. Nedelchev, K. Gyurova, M. Zagorcheva, J. Anal. Appl. Pyrol., 81, 253 (2008).
38. P. Noisong, C. Danavirutai, T. Boonchom, Solid State Sci., 10, 1598 (2008).

\*\*\*\*\*

#### How to cite this article:

El Kababi K *et al.* 2016, Chemical Preparation, Thermal Behavior, Kinetic, ir Studies of  $\text{CdK}_4(\text{P}_3\text{O}_9)_2 \cdot 2\text{H}_2\text{O}$ , Crystallographic Data of a new Cyclotriphosphate  $\text{CdK}_4(\text{P}_3\text{O}_9)_2$  new Fertilizer Type KP. *Int J Recent Sci Res.* 7(6), pp. 11793-11800.

T.SSN 0976-3031



9 770976 303009 >